Tectonophysics 612–613 (2014) 97–105

Contents lists available at ScienceDirect

Tectonophysics

journal homepage: www.elsevier.com/locate/tecto

Magmatic evolution of the Western Myanmar Arc documented by U–Pb and Hf isotopes in detrital zircon

Jian-Gang Wang [a,*], Fu-Yuan Wu [a], Xiu-Cheng Tan [b], Chuan-Zhou Liu [a]

[a] State Key Laboratory of Lithospheric Evolution, Institute of Geology and Geophysics, Chinese Academy of Sciences, Beijing 100029, China
[b] State Key Laboratory of Oil and Gas Geology and Exploitation, School of Resource and Environment, Southwest Petroleum University, Chengdu 610500, China

ARTICLE INFO

Article history:
Received 29 October 2013
Received in revised form 26 November 2013
Accepted 29 November 2013
Available online 10 December 2013

Keywords:
Western Myanmar Arc
Magmatic history
Detrital zircon
U–Pb geochronology
Hf isotope

ABSTRACT

The evolution of the magmatic arc formed along the Asian margin of Neo-Tethys is a key to understand India–Asia convergence. In contrast to the well studied trans-Himalayan magmatic rocks in Tibet, the southeast extension of the arc is still poorly documented in Myanmar, where it is largely buried by sedimentary rocks. This study investigates the magmatic evolution of the western Myanmar arc and the potential along-strike variation of subduction-related magmatism by analyzing U–Pb and Hf isotopes of detrital zircons from the Chindwin Basin in western Myanmar. Our data indicate that the Western Myanmar Arc (WMA) experienced a long-lasting magmatism since the Early Cretaceous, with a main magmatic stage between 110 and 80 Ma and a subordinate magmatic stage at ~70–40 Ma. Arc-derived detrital zircons yield positive $\varepsilon_{Hf}(t)$ values and young model ages (0.1–1.2 Ga), indicating magma generation from a juvenile source. Such geochronologic and geochemical signatures compare well with those of the Kohistan-Ladakh-Gangdese arc in Tibet, indicating uniform magmatic-arc activity all along the Asian margin of Neo-Tethys.

1. Introduction

The vast Tibetan plateau and the Himalayan Orogen were produced during Paleogene collision between the Indian and Asian continents, preceded by prolonged northward subduction of Neo-Tethyan oceanic lithosphere (Hodges, 2000; Yin and Harrison, 2000). An Andean-type magmatic arc over 3000 km in length (the Kohistan-Ladakh-Gangdese-Myanmar arc) has formed along the Asian margin as a result of continuous subduction of the Tethyan slab (Fig. 1A). A comprehensive knowledge of its evolution is vital not only to understand the Neo-Tethyan subduction history, but also to provide the initial conditions necessary to constrain geodynamic models of the Himalayan-Tibetan orogenic system.

Geochronologic and geochemical data from the Kohistan-Ladakh-Gangdese arc in Tibet indicate that most magmatic rocks were formed during Early Cretaceous–Paleogene time, and were derived from very juvenile magma source (Chu et al., 2006, 2011; Ji et al., 2009; Lee et al., 2009; Ravikant et al., 2009; Wen et al., 2008). Its prolongation southeast of the Namche-Barwa syntaxis has not been documented equally well, because the region close to the China–India border is hardly accessible, and magmatic rocks are dislocated by tectonic movements and covered by sedimentary rocks in Myanmar (Fig. 1B). The limited data available from the Western Myanmar Arc (WMA) suggest a geochemical similarity to the Gangdese arc (Mitchell et al., 2012; United Nations, 1978a, 1978b), but its detailed magmatic history is poorly known.

Zircon, a common accessory mineral in igneous rocks, has high durability in weathering and diagenetic processes. The original isotopic signature of the host rocks, therefore, can be preserved in detrital grains during the sedimentary cycle. In this study, we have carried out systematic U–Pb and Lu–Hf isotopic analyses of detrital zircons from the Cretaceous–Miocene strata in the Chindwin Basin, Western Myanmar. Our purpose is to document the sedimentary provenance firstly, and then investigate the magmatic evolution of the WMA and potential along-strike variation of the subduction-related magmatic rocks east of the eastern Himalayan syntaxis.

2. Geological background

The Tibetan Plateau and its southward-flanking Himalayan Orogen developed during northward subduction of Indian Neotethyan lithosphere beneath the Eurasian plate. The Indus–Yarlung-Zangbo suture zone marks the contact between the Indian and Eurasian continental margins (Fig. 1A). North of the suture, the widely developed granitoids in southern Tibet, termed the 'trans-Himalayan batholiths' (Searle et al., 1987), can be subdivided into two principal magmatic belt (Fig. 1A): (1) the southern magmatic belt of Gangdese affinity (Kohistan-Ladakh-Gangdese batholiths) consists dominantly of Early Cretaceous to Eocene I-type granitoids derived from very juvenile source (e.g., Chu et al., 2006; Ji et al., 2009; Zhu et al., 2011), and (2) the northern magmatic belt of central Lhasa affinity comprises

* Corresponding author. Tel.: +86 10 82998547.
E-mail address: wangjiangang@mail.iggcas.ac.cn (J.-G. Wang).

0040-1951/$ – see front matter © 2013 Elsevier B.V. All rights reserved.
http://dx.doi.org/10.1016/j.tecto.2013.11.039

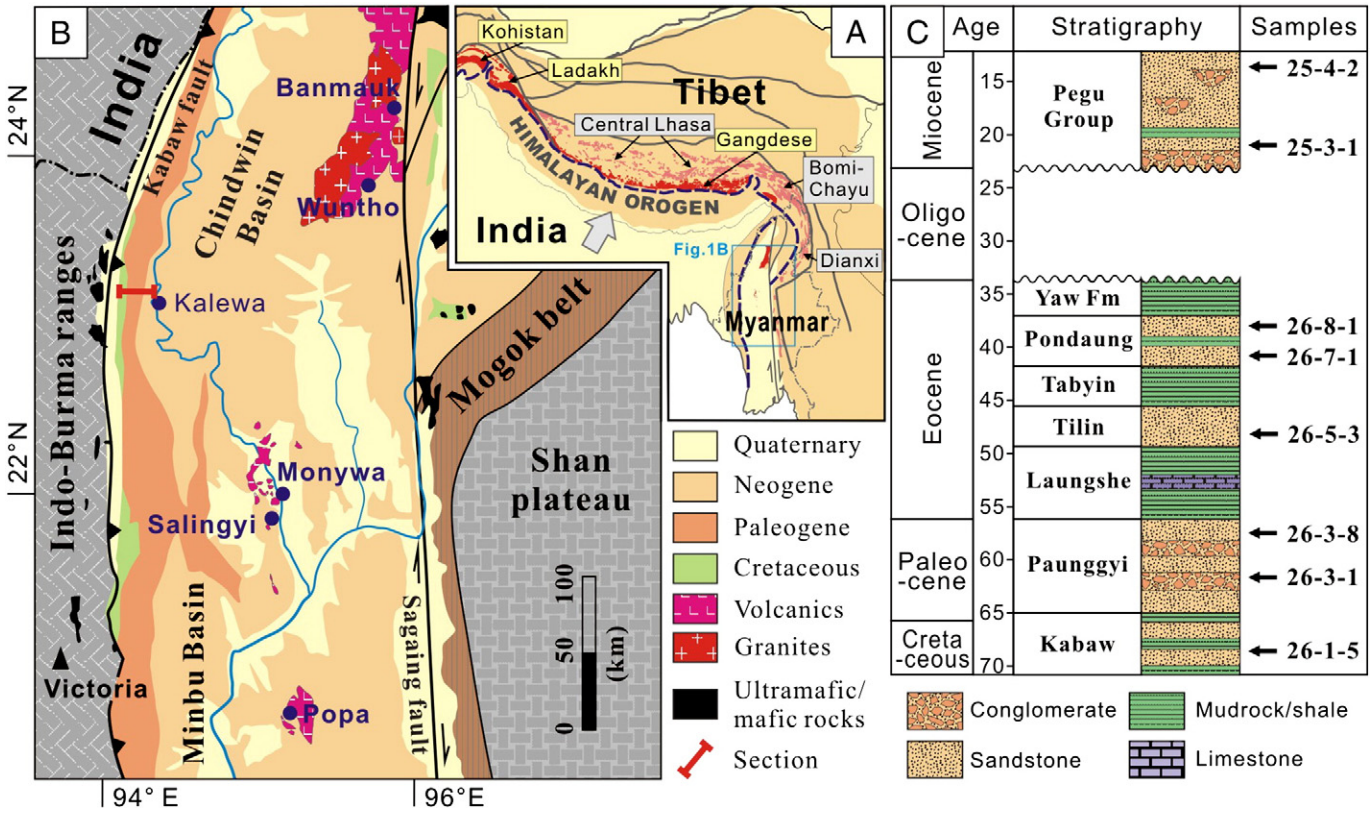

Fig. 1. A: Simplified tectonic map of the Tibetan plateau and adjacent regions, showing localities of the trans-Himalayan batholiths, which comprise the Kohistan-Ladakh-Gangdese magmatic belt in the south and the Central Lhasa-Bomi-Chayu-Dianxi magmatic belt in the north; dashed line indicates the Indus–Yarlung-Zangbo suture zone. B: Geological map of northern Myanmar, showing the studied section near Kalewa (adapted from Bender, 1983). The Western Myanmar arc is delineated by the Banmauk-Wuntho-Monywa-Popa magmatic belt. C: Upper Cretaceous–Lower Miocene succession in the Kalewa section, showing stratigraphic positions of sandstone samples for detrital zircon analyses.

dominantly Early Cretaceous peraluminous and S-type granitoids derived from an old crustal source (Chiu et al., 2009; Kapp et al., 2005; Zhu et al., 2011).

Myanmar is located on the eastern prolongation of the Himalayan orogenic system (Fig. 1A). It comprises four major tectonic domains, from east to west (Fig. 1B): (1) The Shan Plateau, which is part of the Sibumasu Terrane and mostly consists of Paleozoic to lower Mesozoic sedimentary rocks (Metcalfe, 2011; Mitchell, 1992). (2) The Mogok Belt, including marbles, schists and gneisses of amphibolite to locally granulite facies intruded by Jurassic and Miocene granitoids (Barley et al., 2003; Mitchell et al., 2007, 2012; Searle et al., 2007). (3) The Burma Terrane, delimited by the dextral Sagaing Fault in the east and by the Kabaw Fault in the west and comprising the median WMA and Tertiary sedimentary basins on both sides (Mitchell, 1993; Stamp, 1922). (4) The Indo-Burman Ranges, including Cretaceous to Eocene turbidites and mélange deposited in the Burma forearc and younger Bengal Fan turbidites recently accreted in the frontal part of the subduction complex (Allen et al., 2008; Garzanti et al., 2013a; Maurin and Rangin, 2009).

The WMA, located in the central part of the Burma terrane, is a N–S trending magmatic belt delineated by the Banmauk-Wuntho Batholith in the north, and the Monywa and Popa Volcanics in the south (thus it is also called the Wuntho-Papa arc; Fig. 1B). Available geochronologic data from this arc gave Early Cretaceous and Neogene ages (Mitchell et al., 2012; United Nations, 1978a, 1978b). The WMA is widely considered as part of the Andean-type continental arc formed along the South Asian margin during the Neo-Tethyan oceanic subduction (Bender, 1983; Mitchell et al., 2012), but its relationship with the trans-Himalayan arc is unclear because of a lack of data. The Chindwin Basin lies west of the WMA, and is regarded as the forearc basin of the WMA (e.g., Wandrey, 2006; Fig. 1B). It was filled by the upper Cretaceous–Eocene shallow marine or deltatic clastic rocks and carbonates, and the unconformably overlying Neogene fluvial sediments (Bender, 1983; Fig. 1C).

3. Analytical methods

Sandstone samples were collected from different stratigraphic horizons of the Upper Cretaceous–Neogene successions along the highway west of Kalewa town (Fig. 1B). Thin-sections were prepared from all samples. Detrital modal analyses were carried out on 12 less altered samples for tectonic setting discrimination (Table DR2). For consistency and accuracy, ~400 points were counted per sample, following the Gazzi–Dickinson point-counting method (Ingersoll et al., 1984).

Detrital zircons were obtained from eight samples (relative stratigraphic positions are shown in Fig. 1C; and GPS position for each sample is given in Table DR1) using a combination of heavy liquid and magnetic separation techniques. Individual zircon grains were handpicked randomly, mounted in epoxy resin and then polished to remove the upper one third of the grain. Cathodoluminescence (CL) images were obtained using a CAMECA electron microprobe to reveal the internal structures of zircons, and for choosing target sites for U–Pb and Hf analyses.

Zircon U–Pb analyses were conducted on an Agilent 7500a Q-ICP–MS equipped with a 193-nm excimer ArF laser ablation system (Geolas Plus). The detailed analytical procedure was described by Xie et al. (2008). A spot diameter of 44 μm was used in this analysis. Raw count rates for ^{29}Si, ^{204}Pb, ^{206}Pb, ^{207}Pb, ^{208}Pb, ^{232}Th and ^{238}U were collected for age determination. The $^{207}Pb/^{206}Pb$ and $^{206}Pb/^{238}U$ ratios were calculated using the GLITTER program, which was then corrected using

the Harvard zircon 91500 as external calibrate (GEMOC, Macquarie University; Griffin et al., 2008). Common Pb corrections were carried out using the method described by Andersen (2002). Age calculations and plotting of concordia diagrams were performed using Isoplot 3.0 (Ludwig, 2003). Results described in this article exclude analyses with >20% discordance. Zircon age interpretations are based on $^{206}Pb/^{238}U$ ages for grains younger than 1000 Ma and $^{207}Pb/^{206}Pb$ ages for grains older than 1000 Ma.

Zircon Hf isotope analysis was carried out on a Neptune Multi-Collector ICP–MS equipped with the Geolas 193 laser-ablation system. Details on instrumental conditions and data acquisition can be found in Wu et al. (2006). Hf isotope analyses were performed on the same sites as the U–Pb analyses, with a slightly larger (d = 60 μm) laser beam size. During analysis, the average $^{176}Hf/^{177}Hf$ ratio of standard zircon Mud Tank was 0.282506 ± 20, consistent with the reported values (Woodhead and Hergt, 2005), thus further external adjustment was not applied to the analytical results.

All analyses were performed at the State Key Laboratory of Lithosphere Evolution, Institute of Geology and Geophysics, Chinese Academy of Sciences. U–Pb and Hf isotopic data are presented in Tables DR3 and DR4.

4. Analytical results

4.1. Sandstone petrology

The Cretaceous–Eocene sandstones in the Chindwin basin are moderately sorted, angular to sub-angular, lithic to lithoquartzose volcaniclastic (Fig. 2A–E). Volcanic rock fragments are predominantly felsitic, with subordinate microlitic (andesitic) and lathwork (basaltic) types. Quartz grains are angular and commonly show uniform extinction; some display embayments indicative of volcanic origin. Feldspar is minor and dominantly plagioclase. Detrital framework of the Cretaceous–Eocene samples indicates a 'magmatic arc provenance', but with a much larger variation of Q/F ratios than expected for classical provenance models of Dickinson (1985; Fig. 3). By contrast, sandstones from the unconformably overlying Miocene strata (Pegu Group) are lithoquartzose, and include subequal amounts of volcanic, sedimentary,

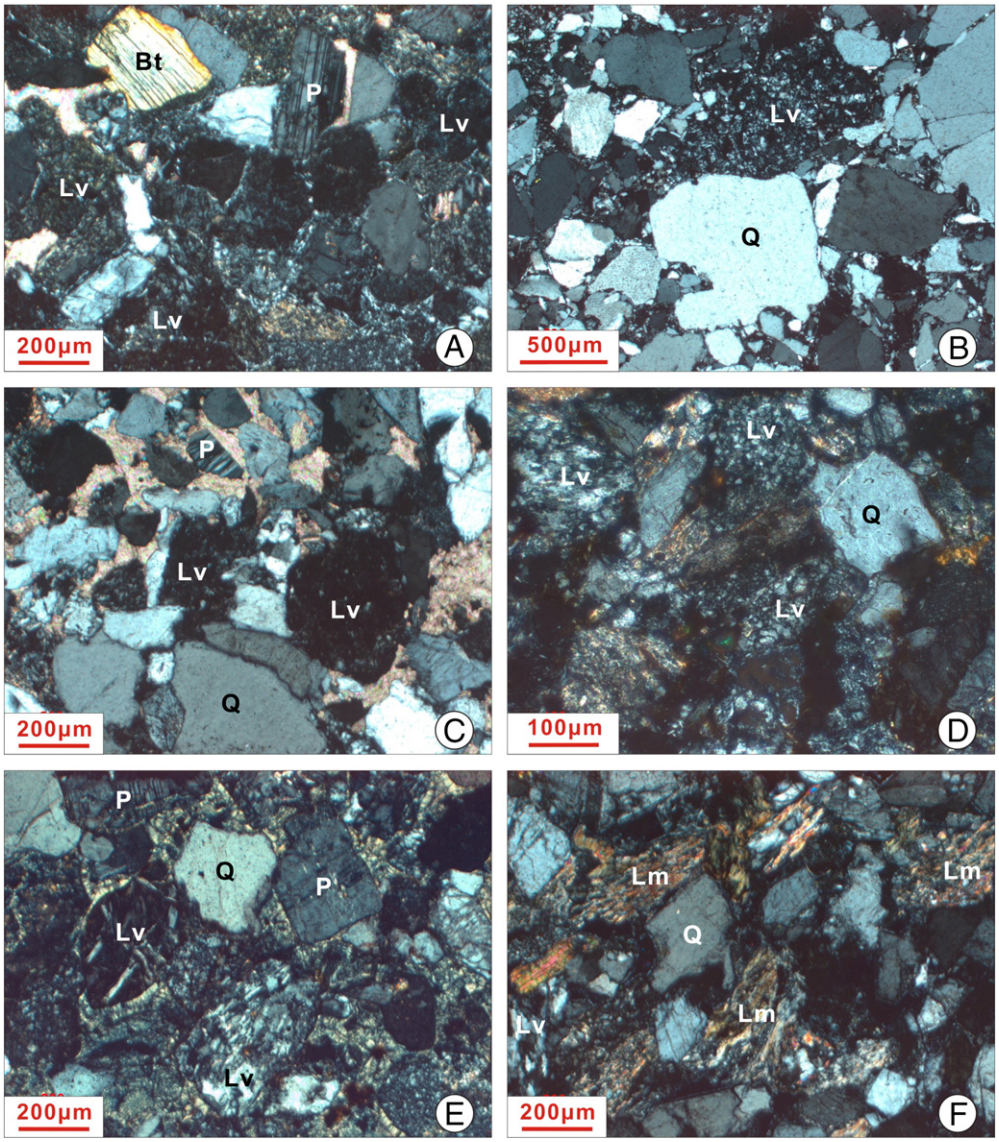

Fig. 2. Petrography of representative sandstone samples from the Chindwin Basin. A: Kabaw Formation; B: Kabaw Formation; C: Paunggyi Formation; D: Tilin Formation; E: Pondaung Formation; F: Pegu Group. Abbreviations: Q, quartz; P, plagioclase; Lv, volcanic rock fragment; Lm, metamorphic rock fragment; Bt, biotite.

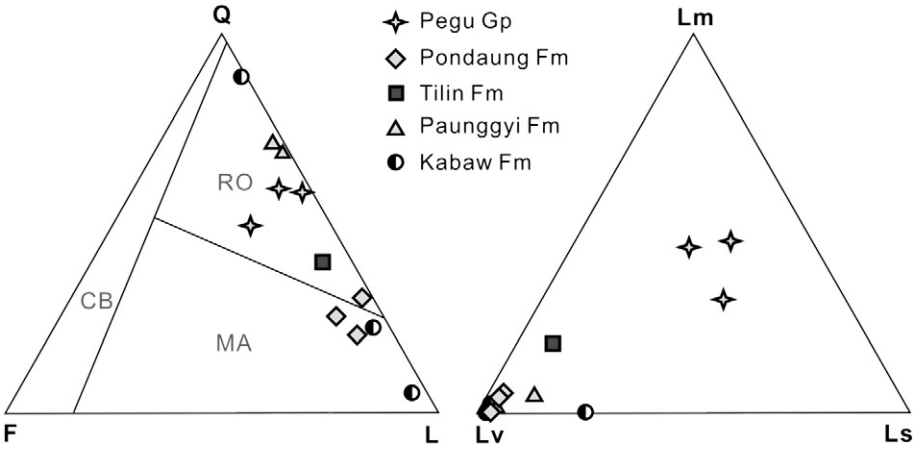

Fig. 3. Petrology of sandstone samples from the Chindwin Basin. Q = quartz, F = feldspar, L = lithic fragments (Lm, metamorphic; Lv, volcanic; Ls, sedimentary). Provenance fields after Dickinson (1985): RO = recycled orogen, CB = continental block, MA = magmatic arc.

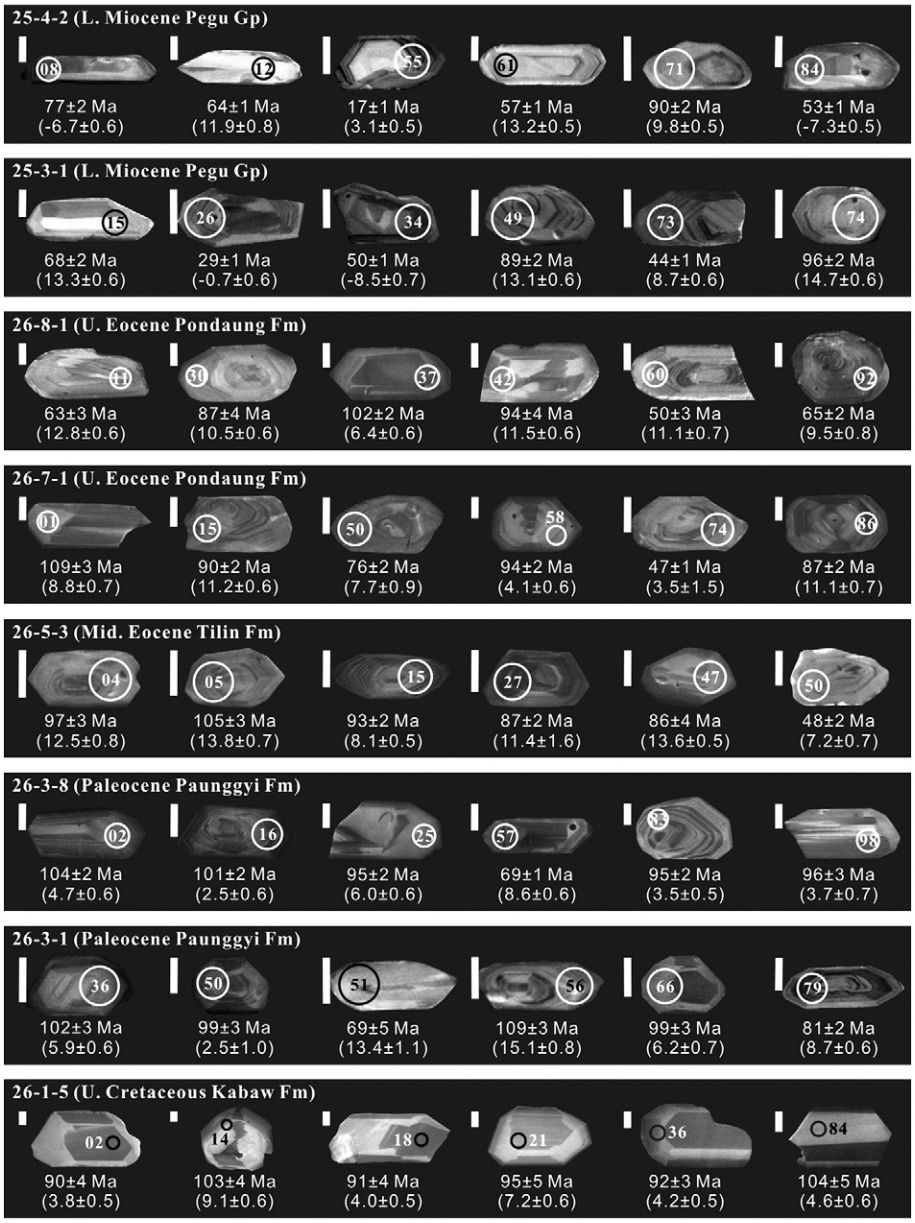

Fig. 4. Representative cathodoluminescence (CL) images of detrital zircons from the Chindwin Basin (scale bar = 50 μm). Circles indicate the positions of LA-ICPMS U–Pb age analyses, d = 44 μm. LA-MC-ICPMS Hf isotope analyses were performed on the same sites with a slightly larger (d = 60 μm) laser beam size. The number in each circle indicates the grain number in the data set.

and metamorphic rock fragments, indicating a mixed orogenic provenance (Garzanti et al., 2007; Fig. 3).

4.2. Zircon U–Pb ages

Detrital zircons from all eight samples are mostly euhedral and have elongated to stout prismatic habits, with length-to-width ratios from 2:1 to 3:1 (Fig. 4). Most zircons are transparent, colorless to pale brown, and show broad to well-developed oscillatory zoning, sector zoning or homogeneous texture in CL images (Fig. 4), indicating that they crystallized from magmas. Zircons with rounded shape and complex internal textures are rare.

One hundred zircon grains were analyzed for each sample. Relative U–Pb age probabilities of detrital zircons are shown in Fig. 6, excluding a few grains that have high discordance (Fig. 5). Zircon age spectra from all samples are dominated by ages that are younger than 200 Ma. Within the <200 Ma ages, most ages cluster at ~110–80 Ma with a notable peak at ~95 Ma. The Paleogene-aged grains increase up-section and become predominant in the Miocene samples, with at ~65 Ma and ~49 Ma. For most samples, the youngest zircon age is very close to their depositional age, indicating continuing volcanic activity in the source area (Fig. 6). In some samples, the >200 Ma ages are abundant, with peaks in the Mesoproterozoic, Neoproterozoic, and Early and Late Paleozoic (Fig. 6).

4.3. Zircon Hf isotopes

Hf isotope analyses were performed on the same grains as the U–Pb analyses. To calculate $\varepsilon_{Hf}(t)$ value and the 'crustal' model age (T_{DM}^{C}), we adopted a depleted mantle model with $^{176}Hf/^{177}Hf = 0.28325$ and $^{176}Lu/^{177}Hf = 0.0384$ (Griffin et al., 2000) and chondrite values for $^{176}Hf/^{177}Hf = 0.282772$ and $^{176}Lu/^{177}Hf = 0.0332$ (BlichertToft and Albarede, 1997). We assumed that the protolith of the zircon's host magma has the average continental crustal $^{176}Lu/^{177}Hf$ ratio of 0.015 (Griffin et al., 2002), and used a decay constant of ^{176}Lu-^{177}Hf of 1.867×10^{-11} per year (Söderlund et al., 2004).

As shown in Fig. 7, the young-aged (<200 Ma) zircons from the Cretaceous–Eocene samples are characterized by positive $\varepsilon_{Hf}(t)$ values. Only in the Paleocene Paunggyi Formation a few grains have slightly negative $\varepsilon_{Hf}(t)$ values. Crustal modal ages of these zircons range from 0.1 to 1.2 Ga. By contrast, abundant young-aged zircons with negative

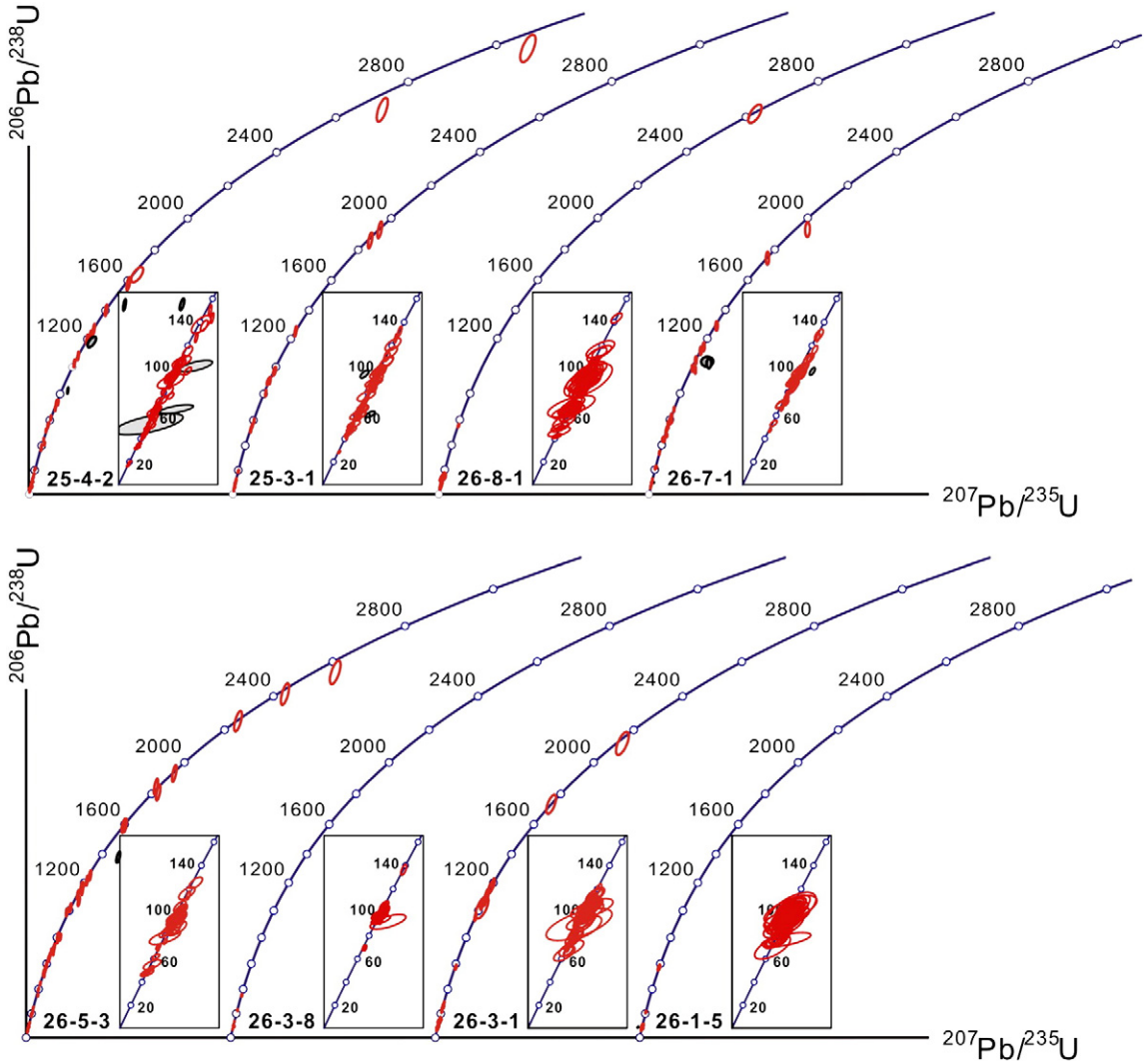

Fig. 5. U–Pb concordia diagrams for detrital zircons from the Chindwin Basin. Ages are in Ma and ellipses show 1σ errors. Analyses in gray are excluded from interpretation because of high discordance.

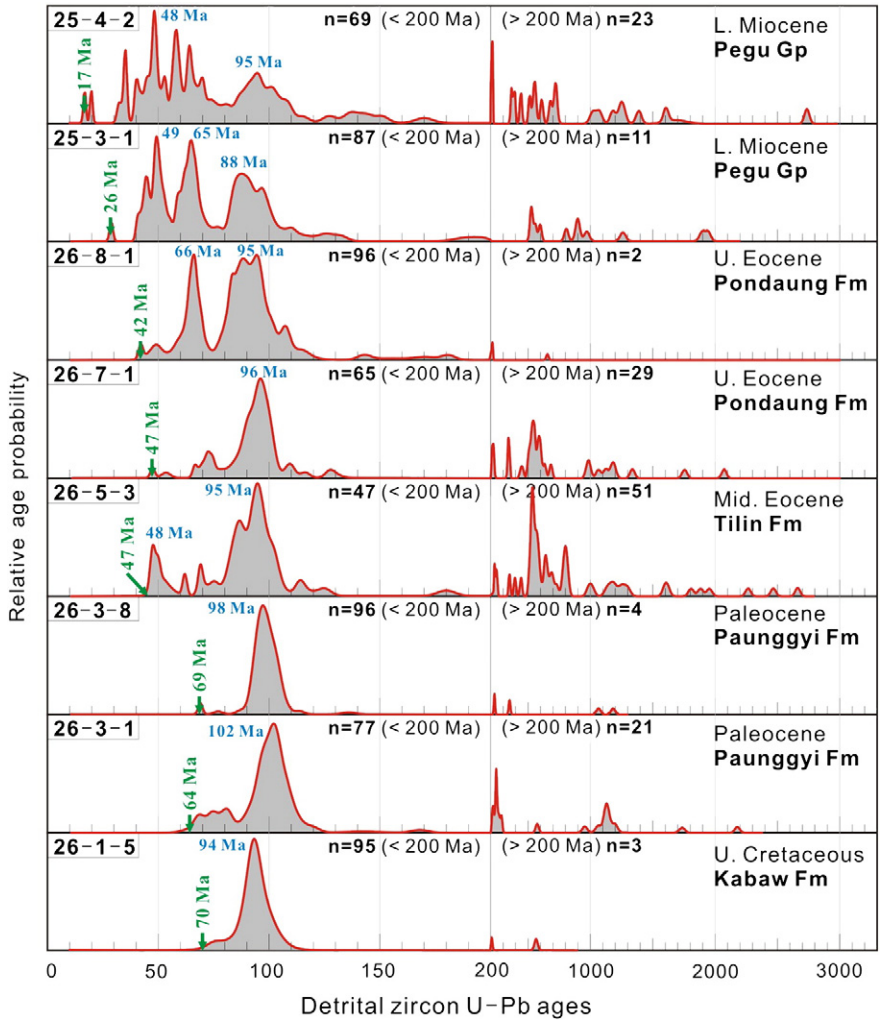

Fig. 6. U–Pb age spectra for detrital zircons from the Upper Cretaceous–Miocene strata in the Chindwin Basin. The youngest zircon age and major age peaks of each sample are indicated.

$\varepsilon_{Hf}(t)$ values occur in the Miocene samples, with crustal modal ages as old as 2.0 Ga (Table DR4).

The old-aged (>200 Ma) zircons from all samples generally have low $^{176}Hf/^{177}Hf$ ratios, with $\varepsilon_{Hf}(t)$ values varying between −34.8 and +9.5, and corresponding crustal modal ages ranging from 1.1 to 3.8 Ga (Table DR4; Fig. 7). A few late Paleozoic–early Mesozoic (~350–200 Ma) zircons have relatively high $^{176}Hf/^{177}Hf$ ratios, with $\varepsilon_{Hf}(t)$ values ranging from +0.5 to +14.7, and crustal modal ages from 0.3 to 1.2 Ga.

5. Discussion

5.1. Sandstone provenance

Dominant volcanic detritus and young-aged zircons in the Upper Cretaceous–Eocene sandstones from the Chindwin Basin indicate the WMA as their proximal 'Magmatic arc' source (Fig. 3; Dickinson, 1985). According to paleogeographic reconstructions, the Chindwin Basin represented the forearc of the WMA, facing Neo-Tethys in the southwest (Wandrey, 2006). The depleted isotopic signature indicated by Hf isotopes of detrital zircons is consistent with the known isotopic features of WMA rocks (Darbyshire and Swainbank, 1988; Mitchell et al., 2012). It excludes provenance from magmatic rocks of the Mogok Belt farther east, which were characterized by enriched isotopic features (Mitchell et al., 2012). The excess of detrital quartz in some samples relatively to purely volcaniclastic sediments (Marsaglia and Ingersill, 1992) is ascribed to recycling of the sedimentary covers of the Burma Terrane, as confirmed by the occurrence of >200 Ma zircons. Alternatively, quartz enrichments may have resulted from equatorial weathering (e.g., Garzanti et al., 2006, 2013b; Smyth et al., 2008).

The presence of abundant sedimentary and metamorphic detritus (Fig. 2F) and young-aged zircons with negative $\varepsilon_{Hf}(t)$ values (Fig. 7) in the Miocene strata indicates significant detrital input from an additional orogenic source. This provenance change is broadly coincident in time with rapid uplift of the Himalayan orogen in the Early Miocene (Harrison et al., 1992; Hodges, 2000; Wang et al., 2013), but we cannot assess whether such additional orogenic source was represented by the Mogok Belt to the east (Mitchell et al., 2012) and/or by the eastern Himalayan syntaxis to the north (Chiu et al., 2009).

5.2. Magmatic evolution of the Western Myanmar Arc

Upper Cretaceous–Paleogene strata of the Chindwin Basin are a reservoir of detritus derived from the WMA, and thus provide useful information to constrain the magmatic evolution of the arc. A summary of U–Pb and Hf isotopic data of young-aged (<200 Ma) zircons from the Cretaceous–Eocene samples is shown in Fig. 8. U–Pb ages of detrital zircons indicate that magmatic activity in the WMA lasted from the Early Cretaceous to the Neogene, with a principal stage between ~110 and 80 Ma and a lesser episode between ~70 and 40 Ma. Such detrital record is consistent with age data from igneous rocks of the WMA. The Banmauk Batholith in the northern WMA has yielded

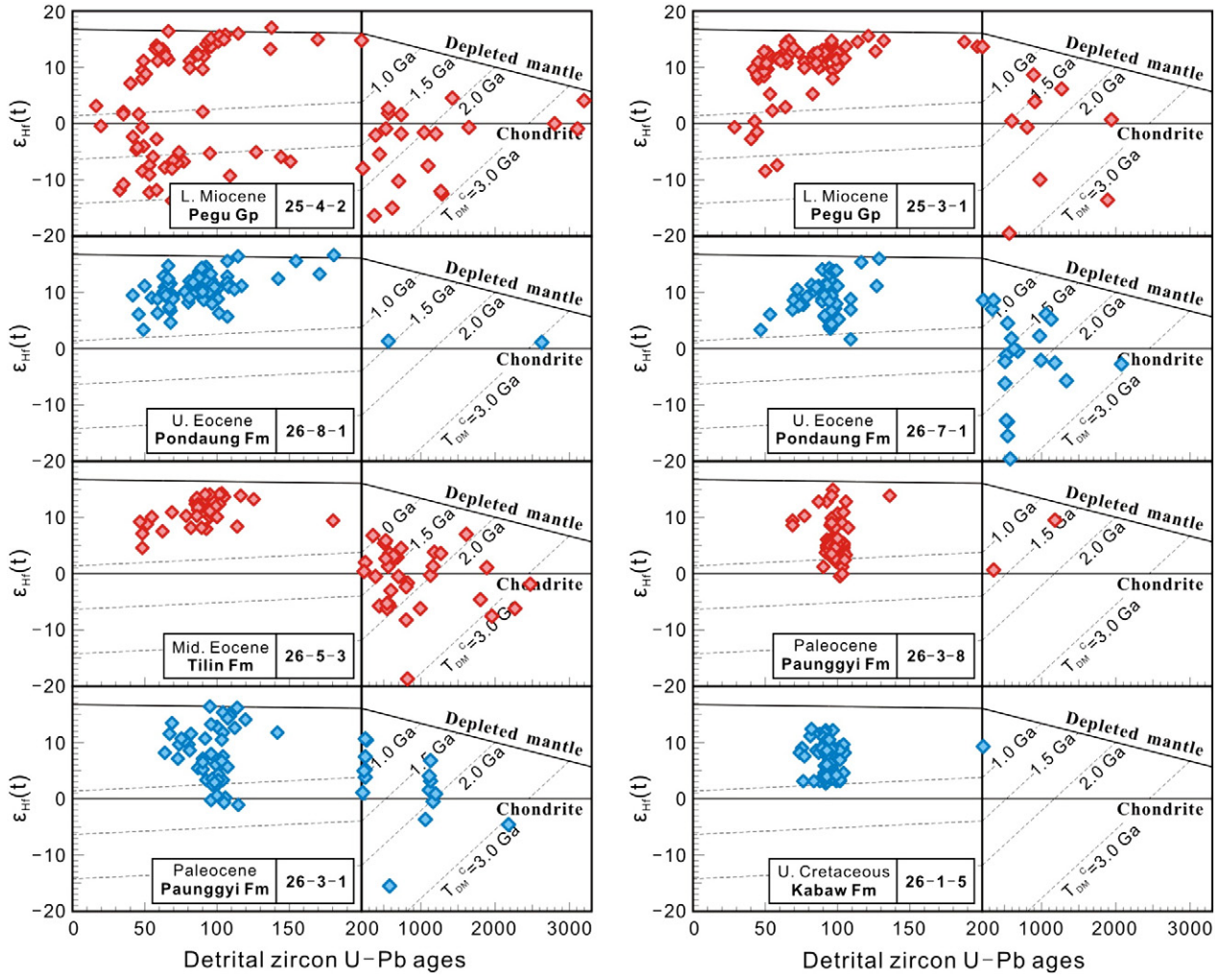

Fig. 7. U–Pb age vs. $\varepsilon_{Hf}(t)$ plots of detrital zircons from the Upper Cretaceous–Miocene strata in the Chindwin Basin.

K–Ar mineral ages of 98–94 Ma (United Nations, 1978a), whereas plutons at Salingyi in the south have given K–Ar ages of 106–91 Ma (United Nations, 1978b) and a zircon U–Pb age of 105 ± 2 Ma (Mitchell et al., 2012).

The arc-derived zircons display positive $\varepsilon_{Hf}(t)$ values corresponding to model ages between 0.1 and 1.2 Ga (Fig. 8), indicating a juvenile magma source for the WMA. This is consistent with Sr–Nd–Hf isotopic fingerprints of WMA rocks. Cretaceous granites in the Banmauk and Salingyi areas (Fig. 1B) have low $^{87}Sr/^{86}Sr$ ratios (0.704–0.705) and positive $\varepsilon_{Nd}(t)$ values (Darbyshire and Swainbank, 1988; Mitchell et al., 2012). Positive $\varepsilon_{Hf}(t)$ values of 7.4–10.8 were also obtained from lower Upper Cretaceous volcaniclastics from the Hukawng valley in northern Myanmar (same sample dated by Shi et al., 2012; Table DR4). Hf isotopic variability in detrital zircons (Fig. 8) may reflect isotopic inhomogeneities of source rocks, possibly caused by different degrees of contamination from an ancient crust.

5.3. Implications

Previous studies have suggested that the WMA might represent the southern continuation of the Mogok Belt, subsequently juxtaposed to the latter by the dextral Sagaing Fault (Mitchell, 1993). More recent data (e.g., Barley et al., 2003; Mitchell et al., 2012; Searle et al., 2007), however, document a different magmatic evolution for the Mogok Belt, which exhibits a long-lasting activity from Jurassic to Miocene and magma generation from enriched sources (Mitchell et al., 2012). Instead, geochronology and geochemical features of the WMA are similar to those of the Gangdese arc in Tibet, yielding pre-Tertiary zircons with U–Pb ages mostly in the 110–80 Ma age range and positive $\varepsilon_{Hf}(t)$ values (Fig. 8). We conclude that the WMA was connected, through the Lohit batholith (Lin et al., 2013), to the Gangdese arc, and formed during subduction of Neo-Tethyan oceanic lithosphere. As suggested by recent works (e.g., Chiu et al., 2009; Mitchell et al., 2012; Xu et al., 2012), the Mogok Belt was linked through the Gaoligong-Bomi-Chayu magmatic belt to the central Lhasa batholiths.

In the Himalayan Orogen, detrital zircon is an effective sedimentary tracer because zircons derived from different tectonic units have different U–Pb ages and Hf isotopes. In previous studies, zircons with positive $\varepsilon_{Hf}(t)$ values found in adjacent basins were considered to have been derived from the Gangdese Arc (e.g., Cina et al., 2009; Hu et al., 2012; Liang et al., 2008). Our new data, indicating that the Gangdese arc continued eastward in the WMA, imply that the latter is an alternative source for these zircons. Thus, some previous provenance interpretations based on detrital zircons may need reconsideration. For instance, detrital zircons with positive $\varepsilon_{Hf}(t)$ values in Upper Miocene sandstones of the Central Burma basin led Liang et al. (2008) to argue that the Yarlung-Zangbo once drained into the Irrawaddy River. Those zircons, however, may well have been derived from the WMA nearby rather than from Gangdese rocks, and therefore connection with the Yarlung-Zangbo River is not proved. Besides, our results have potential implications for tracing detritus from the WMA in the Indo-Burman Ranges, and possibly the Bengal Fan.

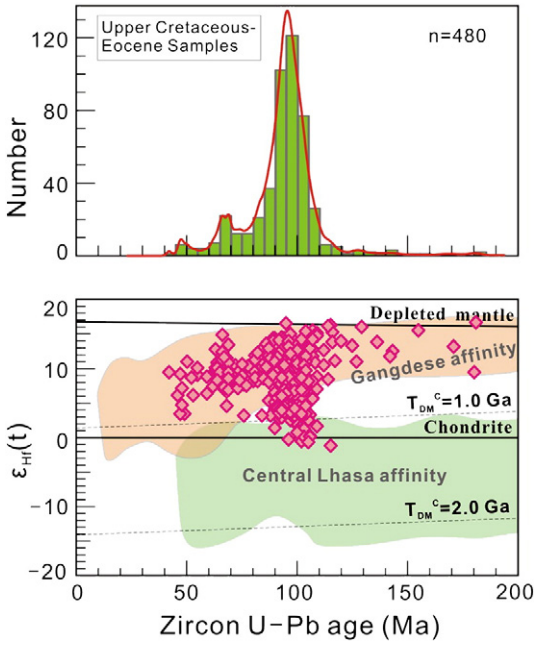

Fig. 8. A summary of U–Pb and Hf isotopic results of Mesozoic–Cenozoic zircons from the Upper Cretaceous–Eocene samples. These zircons were mainly derived from the Western Myanmar Arc and their U–Pb and Hf isotopic characteristics reveal the magmatic history of the latter. Field for magmatic rocks of the 'Gangdese' affinity (Kohistan-Ladakh-Gangdese-Lohit belt, data mainly from Chu et al., 2006; Ji et al., 2009; Lin et al., 2013; Ravikant et al., 2009) and 'Central Lhasa' affinity (Central Lhasa-Bomi-Chayu-Dianxi belt, data mainly from Chiu et al., 2009; Xu et al., 2012; Zhu et al., 2011) are shown for comparison.

6. Conclusion

U–Pb and Hf isotopes of detrital zircons from the forearc strata of the Chindwin Basin revealed that the Western Myanmar Arc has experienced a major volcanic activity during 110–80 Ma and a subordinate magmatic episode at ~70–40 Ma, with magma derived from a very juvenile source. The isotopic features are similar to those of the Kohistan-Ladakh-Gangdese arc in Tibet, indicating that a uniform magmatic arc has formed all along the south Asian margin during the Neo-Tethyan subduction. Our new results have potential implications for tectono-magmatic reconstruction and paleodrainage studies in the eastern Himalayan Orogen.

Supplementary data to this article can be found online at http://dx.doi.org/10.1016/j.tecto.2013.11.039.

Acknowledgements

We thank Yue-Heng Yang and Zhi-Chao Liu for help in zircon U–Pb and Hf isotopic analyses. The manuscript benefited from constructive comments from the editor and Eduardo Garzanti. This work was financially supported by the Key Strategic Project of Chinese Academy of Sciences (XDB03010100) and the National Science and Technology Major Project of China (2011ZX05030-002).

References

Allen, R., Najman, Y., Cater, A., Barfod, D., Bickle, M.J., Chapman, H.J., Garzanti, E., Vezzoli, G., Andò, S., Parrish, R.R., 2008. Provenance of the Tertiary sedimentary rocks of the Indo-Burman Ranges, Burma (Myanmar): Burman arc or Himalayan-derived? J. Geol. Soc. Lond. 165, 1045–1057.

Andersen, T., 2002. Correction of common lead in U–Pb analyses that do not report ^{204}Pb. Chem. Geol. 192, 59–79.

Barley, M.E., Pickard, A.L., Zaw, Khin, Rak, P., Doyle, M.G., 2003. Jurassic–Miocene magmatism and metamorphism in the Mogok metamorphic belt and the India–Eurasia collision in Myanmar. Tectonics. http://dx.doi.org/10.1029/2002TC001398.

Bender, F., 1983. Geology of Burma. Borntraeger, Berlin (293 pp.).

BlichertToft, J., Albarede, F., 1997. The Lu–Hf isotope geochemistry of chondrites and the evolution of the mantle–crust system. Earth Planet. Sci. Lett. 148 (1–2), 243–258.

Chiu, H.Y., Chung, S.L., Wu, F.Y., Liu, D.Y., Liang, Y.H., Lin, I.J., Lizuka, Y., Xie, L.W., Wang, Y.B., Chu, M.F., 2009. Zircon U–Pb and Hf isotopic constraints from eastern Transhimalayan batholiths on the precollisional magmatic and tectonic evolution in southern Tibet. Tectonophysics 477 (1–2), 3–19.

Chu, M.F., Chung, S.L., Song, B.A., Liu, D.Y., O'Reilly, S.Y., Pearson, N.J., Ji, J.Q., Wen, D.J., 2006. Zircon U–Pb and Hf isotope constraints on the Mesozoic tectonics and crustal evolution of southern Tibet. Geology 34 (9), 745–748.

Chu, M.F., Chung, S.L., O'Reilly, S.Y., Pearson, N.J., Wu, F.Y., Li, X.H., Liu, D.Y., Ji, J.Q., Chu, C.H., Lee, H.Y., 2011. India's hidden inputs to Tibetan orogeny revealed by Hf isotopes of Transhimalayan zircons and host rocks. Earth Planet. Sci. Lett. 307 (3–4), 479–486.

Cina, S.E., Yin, A., Grove, M., Dubey, C.S., Shukla, D.P., Lovera, O.M., Kelty, T.K., Gehrels, G.E., Foster, D.A., 2009. Gangdese arc detritus within the eastern Himalayan Neogene foreland basin: implications for the Neogene evolution of the Yalu–Brahmaputra River system. Earth Planet. Sci. Lett. 285 (1–2), 150–162.

Darbyshire, D.P.F., Swainbank, I.G., 1988. Geochronology of a selection of granites from Burma. NERC Isotope Geology Centre Report No 88/6.

Dickinson, W.R., 1985. Interpreting provenance relations from detrital modes of sandstones. In: Zuffa, G.G. (Ed.), Provenance of arenites. NATO Advanced Studies Institute Series, 148. Reidel, Dordrecht, pp. 333–361.

Garzanti, E., Andò, S., Vezzoli, Giovanni, Megid, A.A.A., Kammar, A.E., 2006. Petrology of Nile River sands (Ethiopia and Sudan): sediment budgets and erosion patterns. Earth Planet. Sci. Lett. 252, 327–341.

Garzanti, E., Doglioni, C., Vezzoli, G., Andò, S., 2007. Orogenic belts and orogenic sediment provenances. J. Geol. 115, 315–334.

Garzanti, E., Limonta, M., Resentini, A., Bandopadhyay, P.C., Najman, Y., Andò, S., Vezzoli, G., 2013a. Sediment recycling at convergent plate margins (Indo-Burman Ranges and Andaman–Nicobar Ridge). Earth Sci. Rev. 123, 113–132.

Garzanti, E., Padoan, M., Andò, S., Resentini, A., Vezzoli, G., Lustrino, M., 2013b. Weathering and relative durability of detrital minerals in equatorial climate: sand petrology and geochemistry in the East African rift. J. Geol. 121, 547–580.

Griffin, W.L., Pearson, N.J., Belousova, E., Jackson, S.E., van Achterbergh, E., O'Reilly, S.Y., Shee, S.R., 2000. The Hf isotope composition of cratonic mantle: LAM–MC–ICPMS analysis of zircon megacrysts in kimberlites. Geochim. Cosmochim. Acta 64 (1), 133–147.

Griffin, W.L., Wang, X., Jackson, S.E., Pearson, N.J., O'Reilly, S.Y., Xu, X.S., Zhou, X.M., 2002. Zircon geochemistry and magma mixing, SE China: in-situ analysis of Hf isotopes, Tonglu and Pingtan igneous complexes. Lithos 61, 237–269.

Griffin, W.L., Powell, W.J., Pearson, N.J., O'Reilly, S.Y., 2008. GLITTER: data reduction software for laser ablation ICP–MS. In: Sylvester, P. (Ed.), Laser ablation–ICP–MS in the earth sciences: current practices and outstanding issues. Mineralogical Association of Canada Short Course, 40, pp. 308–311.

Harrison, T.M., Copeland, P., Kidd, W.S.F., Yin, A., 1992. Raising Tibet. Science 255, 1663–1670.

Hodges, K.V., 2000. Tectonics of the Himalaya and southern Tibet from two perspectives. Geol. Soc. Am. Bull. 112 (3), 324–350.

Hu, X.M., Sinclair, H.D., Wang, J.G., Jiang, H.H., Wu, F.Y., 2012. Late Cretaceous–Palaeogene stratigraphic and basin evolution in the Zhepure Mountain of southern Tibet: implications for the timing of India–Asia initial collision. Basin Res. 24 (5), 520–543.

Ingersoll, R.V., Fullard, T.F., Ford, R.L., Grimm, J.P., Pickle, J.D., Sares, S.W., 1984. The effect of grain size on detrital modes: a test of the Gazzi–Dickinson point-counting method. J. Sediment. Res. 54 (1), 103–116.

Ji, W.Q., Wu, F.Y., Chung, S.L., Li, J.X., Liu, C.Z., 2009. Zircon U–Pb geochronology and Hf isotopic constraints on petrogenesis of the Gangdese batholith, southern Tibet. Chem. Geol. 262 (3–4), 229–245.

Kapp, J.L.D., Harrison, T.M., Kapp, P., Grove, M., Lovera, O.M., Ding, L., 2005. Nyainqentanglha Shan: a window into the tectonic, thermal, and geochemical evolution of the Lhasa block, southern Tibet. J. Geophys. Res. 110, B08413. http://dx.doi.org/10.1029/2004JB003330.

Lee, H.Y., Chung, S.L., Lo, C.H., Ji, J.Q., Lee, T.Y., Qian, Q., Zhang, Q., 2009. Eocene Neotethyan slab breakoff in southern Tibet inferred from the Linzizong volcanic record. Tectonophysics 477 (1–2), 20–35.

Liang, Y.H., Chung, S.L., Liu, D.Y., Xu, Y.G., Wu, F.Y., Yang, J.S., Wang, Y.B., Lo, C.H., 2008. Detrital zircon evidence from Burma for reorganization of the eastern Himalayan river system. Am. J. Sci. 308, 618–638.

Lin, T.H., Chung, S.L., Kumar, A., Wu, F.Y., Chiu, H.Y., Lin, I.J., 2013. Linking a prolonged Neo-Tethyan magmatic arc in South Asia: Zircon U–Pb and Hf isotopic constraints from the Lohit Batholith, NE India. Terra Nova. http://dx.doi.org/10.1111/ter.12056.

Ludwig, K., 2003. User's Manual for Isoplot 3.00: A Geochronological Toolkit for Microsoft Excel (Kenneth R. Ludwig).

Marsaglia, K.M., Ingersill, R.V., 1992. Compositional trends in arc-related, deep-marine sand and sandstone: a reassessment of magmatic-arc provenance. Geol. Soc. Am. Bull. 104 (12), 1637–1649.

Maurin, T., Rangin, C., 2009. Structure and kinematics of the Indo-Burmese Wedge: recent and fast growth of the outer wedge. Tectonics 28 (2), TC2010. http://dx.doi.org/10.1029/2008TC002276.

Metcalfe, I., 2011. Tectonic framework and Phanerozoic evolution of Sundaland. Gondwana Res. 19 (1), 3–21.

Mitchell, A.H.G., 1992. Late Permian–Mesozoic events and the Mergui Group nappe in Myanmar and Thailand. J. SE Asian Earth Sci. 7 (2–3), 165–178.

Mitchell, A.H.G., 1993. Cretaceous–Cenozoic tectonic events in the western Myanmar (Burma)–Assam region. J. Geol. Soc. Lond. 150 (6), 1089–1102.

Mitchell, A.H.G., Htay, M.T., Htun, K.M., Win, M.N., Oo, T., Hlaing, T., 2007. Rock relationships in the Mogok metamorphic belt, Tatkon to Mandalay, central Myanmar. J. Asian Earth Sci. 29 (5–6), 891–910.

Mitchell, A., Chung, S.L., Oo, T., Lin, T.H., Hung, C.H., 2012. Zircon U–Pb ages in Myanmar. Magmatic–metamorphic events and the closure of a neo-Tethys ocean? J. Asian Earth Sci. 56, 1–23.

Ravikant, V., Wu, F.Y., Ji, W.Q., 2009. Zircon U–Pb and Hf isotopic constraints on petrogenesis of the Cretaceous–Tertiary granites in eastern Karakoram and Ladakh, India. Lithos 110 (1–4), 153–166.

Searle, M.P., Windley, B.F., Coward, M.P., Cooper, D.J.W., Rex, D., Li, T., Xiao, X., Jan, M.Q., Thakur, V.C., Kumar, S., 1987. The closing of Tethys and the tectonics of Himalaya. Geol. Soc. Am. Bull. 98, 678–701.

Searle, M.P., Noble, S.R., Cottle, J.M., Waters, D.J., Mitchell, A.H.G., Hlaing, Tin, Horstwood, M.S.A., 2007. Tectonic evolution of the Mogok Metamorphic belt, Burma (Myanmar) constrained by U–Th–Pb dating of metamorphic and magmatic rocks. Tectonics 26, TC3014. http://dx.doi.org/10.1029/2006TC002083.

Shi, G.H., Grimaldi, D.A., Harlow, G.E., Wang, J., Wang, J., Yang, M.C., Lei, W.Y., Li, Q.L., Li, X.H., 2012. Age constraint on Burmese amber based on U–Pb dating of zircons. Cretac. Res. 37, 155–163.

Smyth, H., Hall, R., Nichols, G.J., 2008. Significant volcanic contribution to some quartz-rich sandstones, East Java, Indonesia. J. Sediment. Res. 78, 335–356.

Söderlund, U., Patchett, P.J., Vervoort, J.D., Isachsen, C.E., 2004. The ^{176}Lu decay constant determined by Lu–Hf and U–Pb isotope systematics of Precambrian mafic intrusions. Earth Planet. Sci. Lett. 219 (3–4), 311–324.

Stamp, L.D., 1922. An outline of the Tertiary geology of Burma. Geol. Mag. 59 (11), 481–501.

United Nations, 1978a. Geology and exploration geochemistry of the Pinlebu-Banmauk area, Sagaing Division, northern Burma. Technical Report No. 2. DP/UN/BUR-72-002. Geological Survey and Exploration Project, United Nations Development Programme, New York (69 pp.).

United Nations, 1978b. Geology and exploration geochemistry of the Salingyi-Shinmataung area, central Burma. Technical Report No. 5. DP/UN/BUR-72-002/14. Geological Survey and Exploration Project, United Nations Development Programme, New York, p. 29.

Wandrey, C.J., 2006. Eocene to Miocene composite total petroleum system, Irrawaddy-Andaman and North Burma Geologic Provinces, Myanmar, Chapter E. In: Wandrey, C.J. (Ed.), Petroleum systems and related geologic studies in Region 8, South Asia. U.S. Geological Survey Bulletin, 2208-E (26 pp.).

Wang, J.G., Hu, X.M., Garzanti, E., Wu, F.Y., 2013. Upper Oligocene–Lower Miocene Gangrinboche conglomerate in the Xigaze Area, Southern Tibet: implications for Himalayan uplift and Paleo-Yarlung-Zangbo initiation. J. Geol. 4, 425–444.

Wen, D.R., Liu, D.Y., Chung, S.L., Chu, M.F., Ji, J.Q., Zhang, Q., Song, B., Lee, T.Y., Yeh, M.W., Lo, C.H., 2008. Zircon SHRIMP U–Pb ages of the Gangdese Batholith and implications for Neotethyan subduction in southern Tibet. Chem. Geol. 252 (3–4), 191–201.

Woodhead, J.D., Hergt, J.M., 2005. Preliminary appraisal of seven natural zircon reference materials for in situ Hf isotope determination. Geostand. Geoanal. Res. 29, 183–195.

Wu, F.Y., Yang, Y.H., Xie, L.W., Yang, J.H., Xu, P., 2006. Hf isotopic compositions of the standard zircons and baddeleyites used in U–Pb geochronology. Chem. Geol. 234, 105–126.

Xie, L.W., Zhang, Y.B., Zhang, H.H., Sun, J.F., Wu, F.Y., 2008. In situ simultaneous determination of trace elements, U–Pb and Lu–Hf isotopes in zircon and baddeleyite. Chin. Sci. Bull. 53, 1565–1573.

Xu, Y.G., Yang, Q.J., Lan, J.B., Luo, Z.Y., Huang, X.L., Shi, Y.R., Xie, L.W., 2012. Temporal–spatial distribution and tectonic implications of the batholiths in the Gaoligong–Tengliang–Yingjiang area, western Yunnan: constraints from zircon U–Pb ages and Hf isotopes. J. Asian Earth Sci. 53, 151–175.

Yin, A., Harrison, T.M., 2000. Geologic evolution of the Himalayan–Tibetan orogen. Annu. Rev. Earth Planet. Sci. 28, 211–280.

Zhu, D.C., Zhao, Z.D., Niu, Y.L., Mo, X.X., Chung, S.L., Hou, Z.Q., Wang, L.Q., Wu, F.Y., 2011. The Lhasa Terrane: record of a microcontinent and its histories of drift and growth. Earth Planet. Sci. Lett. 301 (1–2), 241–255.